Onset of Rotating Disturbance in the Interelectrode Region and Exhaust Jet of an MPD Arc

FRANK ALLARIO,* OLIN JARRETT JR.,† AND ROBERT V. HESS‡
NASA Langley Research Center, Hampton, Va.

Experimental results are presented of a parametric study of the onset of rotating disturbances ($f \leq 500$ kHz) in the plasma of a 15 to 40 kw MPD arc. Measurements were taken in the exhaust and interelectrode regions, using optical and electrostatic probes. The dependence of critical magnetic field (B_c) on mass flow, background pressure, and propellant are given. In argon, B_c varied from 800 to 1800 gauss for a mass flow change of 14 to 100 mg/sec. Considerably higher values of B_c were obtained in xenon. Little dependence on background pressure was found. Diagnostics were performed on the quiet preonset and the postonset plasma states. The latter evolved from a coherent disturbance at low B to an apparent turbulent state at high B. Thrust measurements in these different plasma states are discussed. The behavior of the onset of the rotating disturbance is similar to that found in a linear Hall current accelerator.

Introduction

THE presence of low-frequency rotating disturbances in a low-power coaxial plasma accelerator, the linear Hall current accelerator, was established several years ago.[1-3] The presence of low-frequency fluctuations in a low-power MPD arc[4] (~1 kw) and a high-power MPD arc[5] (15–25 kw) were also indicated several years ago, and the suggestion was made at that time[5] that the disturbances in the MPD arc and linear Hall accelerator were similar.

More recently a study of rotating disturbances in a high-power MPD arc was conducted under quasi-steady operation using electrostatic and Rogowski coil probes to detect the disturbance.[6] Measurements of the internal current distribution established the presence of rotating disturbances in the device. Rotational disturbances in a steady high-power MPD arc were recently reported by Larson using a segmented anode[7] and by Connolly et al., using Rogowski coil probes.[8]

However, these results did not answer the important question whether the disturbance already exists at zero applied magnetic field like an arc spoke which is merely rotated in the presence of an externally applied magnetic field or whether the disturbance onsets at a finite critical magnetic field B_c, like an instability. The existence of an onset was recently reported for a low-power linear Hall accelerator by Sidney et al.,[9] and the existence of a disturbance onset in the exhaust jet of a high-power MPD arc was also recently reported by Malliaris.[10]

One purpose of the present paper is to present results of an experimental parametric study of rotating disturbances in a high-power MPD arc (15–40 kw) to determine whether onset of the disturbance occurs throughout the entire device (interelectrode and exhaust region) and to evaluate the dependence of B_c on mass flow, propellant, and current. A comparison with a similar study in the linear Hall accelerator is also made since the behavior of the rotating disturbance in the two devices is strikingly similar. Using an externally heated cathode, the linear Hall accelerator of Ref. 9 has been operated up to 10 amp so that the usefulness of such a comparison is more meaningful.

Another purpose of the paper is to present results of the behavior of the rotating disturbance in the high-power MPD arc in preonset and postonset operation using electrostatic probing, streak photography, and spectroscopic measurements of the emitted light intensity. These results are compared with thrust measurements performed when the arc plasma was stable (preonset) and unstable (postonset), and the relative merit of operating a high-power MPD arc efficiently at high B is discussed.

Apparatus and Instrumentation

A schematic of the MPD arc is shown in Fig. 1. The cathode was a $\frac{3}{8}$-in.-diam, 2% thoriated tungsten rod employing a tapered tip. The cathode extended out from the rear insulator $\frac{7}{8}$ in. The anode, which was partly radiation-cooled, was machined from a copper-impregnated tungsten cylinder (16% Cu and 84% W). The internal diameter of the anode was $\frac{7}{8}$ in. and the length was 1 in.

Eight $\frac{1}{16}$-in.-diam drill-through holes in the anode allowed injection of mass flow into the discharge gap through the anode. The propellant could also be injected through the insulator in the rear of the cathode. The mass flow ($\dot{m}$) was varied from 14 to 100 mg/sec. Most measurements were obtained using argon as propellant, but other gases were studied including helium, xenon, nitrogen, and ammonia. For $\dot{m}$ in argon less than 20 mg/sec, the background tank pressure was maintained below 5 mtorr. For $\dot{m}$ greater than 20 mg/sec, the tank pressure never exceeded 70 mtorr.

Standard motor generator sets were used to supply the arc power. The current ranged from 300 to 600 amp. An almost uniform axial magnetic field B was maintained in the interelectrode region by an external magnetic field coil, with B diverging downstream of the electrodes. The reported values of B are those at the cathode tip, where B was varied between 250 and 5000 gauss.

Electrostatic probing and optical measurements were used to detect the presence of the rotating disturbance in the arc plasma. The frequency spectrum of oscillations in the floating potential and in the ion saturation current collected by conventional Langmuir probes made of tungsten were displayed on a Panoramic Spectrum Analyzer in the frequency range 0–700 kHz. This frequency range was ex-

Presented as Paper 69-232 at the AIAA 7th Electric Propulsion Conference, Williamsburg, Va., March 3–5, 1969; submitted April 1, 1969; revision received October 1, 1969.

* Aero-Space Technologist, Plasma Physics and Gas Laser Branch, Aero-Physics Division.

† Aero-Space Technologist, Plasma Physics and Gas Laser Branch, Aero-Physics Division. Associate Fellow AIAA.

‡ Head, Plasma Physics and Gas Laser Branch, Aero-Physics Division. Associate Fellow AIAA.

tended up to 1 MHz using a Tektronix-type 1L5 spectrum analyzer.

For measurements in the interelectrode region, the tungsten probes became excessively hot (and probably emitting) so that probe measurements in this region were supplemented by taking streak photographs of the emitted light using an STL image converter camera. Optical stops limited the light examined to that in the interelectrode region. Spectroscopic measurements of the light intensity were obtained with a $\frac{1}{2}$-m grating spectrometer. The light intensity at the output slit of the spectrometer was detected by a 1P21 photomultiplier tube. Spectroscopic measurements were made using a side-on view of the exhaust beam, 3 in. downstream of the anode.

Thrust measurements were performed by monitoring the axial deflection of a 4-in.-diam boron nitride disk, positioned 4 in. downstream of the anode. The disk was positioned so its centerline was aligned perpendicular to the central axis of the accelerator. The disk was mounted on a moment arm whose deflection was measured by a strain gage. The output of the strain gage was fed into a low-frequency response galvanometer in a CEC 124 oscillograph. Calibration of the system was performed with precision weights and the system had a linear response. The accuracy of this method of thrust determination is not ideal, but it was chosen since it does give a relatively simple way to obtain a gross indication of the variation in thrust for various operating conditions, in particular thrust vs magnetic field.

Experimental Results and Discussion

Electrostatic Measurements near B_c and for $B > B_c$

In Fig. 2 the frequency spectrum of floating potential oscillations 3 in. downstream of the anode is shown for four values of B. The mass flow was 32 mg/sec and was injected between the electrodes, but injection of mass flow through the anode did not appreciably alter the results. A mass flow of 32 mg/sec was chosen to exhibit the behavior of the rotating disturbance with B, since for this mass flow the rotating disturbance exhibits a relatively high signal-to-noise ratio for relatively high values of B, and thus serves as a good example of the behavior of the rotating disturbance over a wide range of B. However, it must be kept in mind that B_c depends upon mass flow. (These results are shown in Fig. 5.) The current for all four conditions was constant at 300 amp.

Below each photograph, the center frequency of the spectrum analyzer frequency window and the strength of B at the cathode tip are shown. The signal at zero frequency is a reference signal internally generated by the spectrum analyzer.

In Fig. 2a where B is 1520 gauss, no disturbance is detected. With a change in B of only 30 gauss (Fig. 2b), a sharp signal appears at 45 kHz with an associated first harmonic at 90 kHz. These photographs show that the disturbance onset occurs somewhere between 1520 and 1550 gauss for 32 mg/sec. Such an abrupt onset was characteristic of the rotating disturbance over the entire range of mass flow examined, and in general B_c could be reproduced to within ± 20 gauss. The primary limitation in reproducing B_c was associated with the sensitivity of the control on the solenoid producing the axial magnetic field. A similar abrupt onset was observed for the ion saturation current 3 in. downstream of the anode.

In Fig. 2c, it is seen that with a further increase in B of only 50 gauss both the amplitude and frequency of the rotating disturbance increase. The frequency of the fundamental is 55 kHz, and the first harmonic is off the range of the spectrum analyzer window of 100 kHz width, but the first harmonic was observed with a wider window. However, a second frequency peak has appeared at 80 kHz. At this value of B, the rotating disturbance takes on the appearance

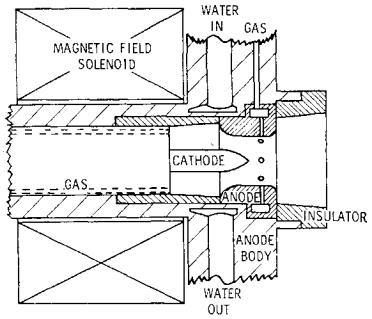

Fig. 1 Schematic of MPD arc.

of a dual frequency instability. In the present experiments using argon as propellant, the dual frequency disturbance was detected for a mass flow up to 40 mg/sec. Above this mass flow the rotating disturbance exhibited a true harmonic structure. Azimuthal phase-shift measurements were performed on both frequency peaks, f_1 and f_2. f_1, the low-frequency signal, was an $m = 1$ mode and f_2, the high-frequency signal, was an $m = 2$ mode. The disturbance rotated in the direction of $\mathbf{j} \times \mathbf{B}$ and reversed direction of rotation when the direction of B was reversed. The presence of dual-frequency disturbances in a low-pressure magnetically confined plasma jet in argon has been reported by Shipp and Dunnill, although their device operated at much lower power levels.[11]

In Fig. 2d, B has been increased to 5500 gauss. The center frequency has been extended to 100 kHz, and the gain increased by a factor of two. For this value of B, f_1 has increased to 100 kHz and exhibits a broad spread in frequency ($\approx$40 kHz). f_2 has increased to 160 kHz and also shows a rather broad spread in frequency.

In Fig. 2d observe the increase by about a factor of five of noncoherent noise oscillations. An analysis of the frequency spectrum of the noncoherent oscillations was made in the range 0–1 MHz. The noncoherent oscillations showed a broad frequency peak between 500 and 600 kHz, which increased in amplitude as B was raised from 3200 to 5000 gauss. The appearance of noncoherent oscillations at some critical B depended upon the mass flow, noncoherent oscillations setting in at higher values of B at higher mass flows. For example, at a mass flow in argon of 14 mg/sec, the amplitude of noncoherent oscillations was comparable to that of the coherent oscillations when B was approximately 2400 gauss while for a mass flow of 32 mg/sec, the amplitudes became comparable when B was approximately 5000 gauss. Above 32 mg/sec, the noncoherent oscillations were not observed for the range of B we examined.

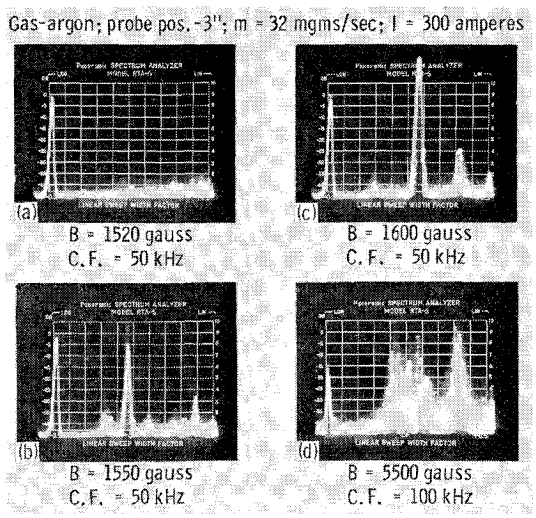

Fig. 2 Onset of rotating instability at 32 mg/sec.

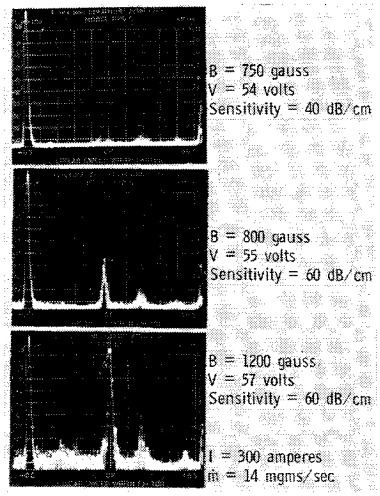

Fig. 3 Onset of rotating instability at 14 mg/sec.

In an effort to determine whether the onset could be detected in the region between the electrodes as well as three in. downstream of the anode, tungsten probes were inserted directly in the interelectrode region and the frequency spectrum of the floating potential oscillations was displayed on the spectrum analyzer. Figure 3 is an example of these results for a mass flow of 14 mg/sec in argon and an arc current of 300 amp. The center frequency was 100 kHz for all three pictures. At 14 mg/sec, the coherent disturbance onsets at approximately 800 gauss and exhibits a dual frequency structure. The lower frequency of this dual frequency structure was almost 100 kHz and the higher frequency was almost 140 kHz. Similar results were obtained with electrostatic probes located 3 in. downstream of the anode with the exception that the signal-to-noise ratio was higher in the interelectrode region by about a factor of five.

Optical Measurements near B_c and for $B > B_c$

Since tungsten probes inserted directly in the region between electrodes became hot within the course of a run, electrostatic probe data in the interelectrode region was supplemented with streak photography, using an STL image converter camera. The results are shown in Fig. 4. In this case the camera was directed upstream with the optic axis of the camera lens aligned directly with the optic axis of the MPD arc. Light emitted by the cathode and anode were masked off and the streak camera examined light emitted in a small portion of the region between the electrodes. A system of optical stops assured that most of the light examined originated in the region between the electrodes. On each photograph, the cathode lies to the left of the streaked image and the anode to the right. Increasing time is in the downward direction, with a streak duration of 50 μsec used in each case. The value of B is given below each photograph. In this particular measurement, the mass flow was 14 mg/sec and arc conditions were the same as those of Fig. 3.

In the first streak photograph in Fig. 4, the distribution of light is uniform indicating a weak or nonexisting nonuniformity (rotating disturbance) in the interelectrode region. As B is further increased by a hundred gauss, faint periodic patterns of light and dark become evident on the streaked image indicating that onset occurs somewhere between 800 and 900 gauss. This streaked image is not shown since it did not reproduce well, but it does confirm electrostatic probe results that onset in the region between electrodes occurs at approximately 800 gauss at 14 mg/sec. Moreover, the faint periodic patterns also agree with the relatively weak amplitude of the rotating disturbance just after onset. When B is further increased to 1200 gauss (second streaked image), well-defined periodic patterns of light and dark appear on the streaked image. (Compare these results with electrostatic probe results shown in Fig. 3.) This shows that a well-formed nonuniformity is present in the region between electrodes, with a frequency of approximately 100 kHz. Further increase of B to 1600 and 3200 gauss (third and fourth streaked images) increases the frequency to 150 and 200 kHz. Above 3200 gauss, the nonuniformity could not be distinguished above the background light emission (probably due to the increase of noncoherent oscillations in the plasma).

These optical measurements just presented are important since they represent direct probing of the interelectrode region of the arc plasma without introducing any perturbation, and establish the existence of a true onset since the disappearance of rotating disturbances in the exhaust jet does not exclude their persistence in the interelectrode region.

Tungsten probes were also positioned as far as 10 in. downstream of the anode and 3 in. off the center axis of the arc. These probes showed the same value of B_c at the cathode tip as the optical measurements and tungsten probes located in the electrode gap. Thus, there appears to be no difference in the magnitude of B_c for the onset either in the interelectrode region or exhaust region, even though the magnetic field distribution differs in the two regions. This suggests that the onset of the rotating disturbance is most likely controlled by plasma conditions in the interelectrode region of the device, similar to what was observed in the linear Hall accelerator of Ref. 8.

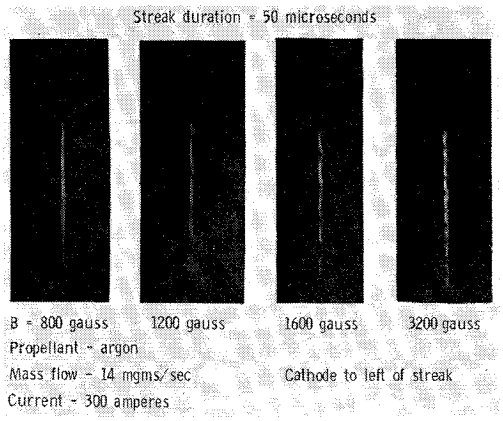

Fig. 4 STL image converter streak photographs.

B_c vs Mass Flow in the MPD Arc

In Fig. 5 the dependence of B_c on mass flow is shown for several propellants. Above each solid line, the plasma is unstable and below each solid line, the plasma is stable. In the lighter propellants (ammonia and nitrogen), B_c shows little dependence on mass flow. In ammonia at 20 mg/sec, B_c was approximately 500 gauss and for nitrogen at the same mass flow, B_c was approximately 750 gauss. B_c was also examined

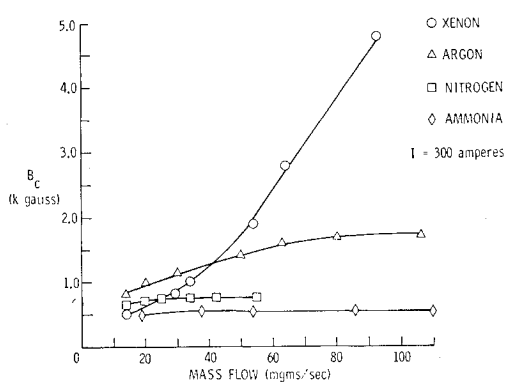

Fig. 5 Critical field vs mass flow in MPD arc.

in helium and showed hardly any dependence on mass flow. Its onset value was always below that of ammonia.

In the heavier inert gases (argon and xenon), B_c showed some dependence on mass flow. In argon, B_c changed from 800 gauss at 14 mg/sec to 1800 gauss at 100 mg/sec. In xenon, B_c showed the greatest dependence on mass flow and for $\dot{m}$ = 100 mg/sec, B_c was as high as 5000 gauss. This behavior seems to imply that B_c depends upon the mass of the propellant, especially if results in argon and xenon are compared. However, the crossover of the two curves at low mass flow (argon and xenon), also implies that this dependence is not a simple one and that the ionization potential of the different gases also plays a role in determining B_c.

An independent check was also conducted to determine what effect, if any, the background tank pressure had on B_c. For a change in background pressure in argon from 0.50 to 100 mtorr, B_c showed little variation; this again suggests that onset of the disturbance is controlled by plasma conditions in the interelectrode region as opposed to those in the exhaust region.

The variation of B_c with mass flow and propellant has been compared to similar results obtained in the linear Hall current accelerator. In Fig. 6 the dependence of B_c on pressure is shown for the linear Hall accelerator as presented in Ref. 9. For the range of parameters shown in Fig. 6, the pressure is linearly related to the mass flow. In the linear device, B_c shows hardly any dependence on mass flow in helium and nitrogen; however, the dependence on mass flow is noticeable for argon and is even more pronounced in xenon. These results, although at a lower mass flow and lower power level, show a striking similarity to those obtained in a 15–40 kw MPD arc, indicated in Fig. 5.

This similarity is significant since it suggests that the nature of rotating disturbances and their onset is similar in the high-power MPD arc and the low-power linear Hall accelerator. In the linear device, it has been established that onset of the rotating disturbance depends critically upon the strength of B within a small region, localized about the thermionically emitting cathode (~5 mm). It was found that onset of the disturbance could be controlled by controlling B to less than B_c in this small region, independent of the strength of magnetic field in the rest of the device. This suggests the possibility of controlling the disturbance onset in the MPD arc by controlling B near the cathode, as was done for the linear Hall accelerator, say by field-shaping of the magnetic field.

B_c vs Current

The dependence of B_c on current was also obtained in the current range between 300 and 500 amp, for $\dot{m}$ in argon between 14 and 65 mg/sec. It was observed that for constant $\dot{m}$, B_c decreased with increasing current although the change was small. For example, with an $\dot{m}$ of 14 mg/sec, B_c decreased from 800 gauss at 300 amp to 500 gauss at 500 amp. However, since this represented a relatively small current variation, the dependence of B_c on the arc current was also obtained in an MPD arc employing a hollow cathode instead of the solid cathode, thus permitting a wider current variation (50 to 600 amp). The hollow cathode was machined from a barium impregnated tungsten rod with an o.d. of 0.50 in. and an i.d. of 0.25 in. (The interelectrode gap was somewhat smaller than the configuration employing the solid cathode so that a direct comparison of results using the two cathodes should not be made.) Within the current range from 50 to 600 amp, B_c decreased with increasing current at constant $\dot{m}$. Specifically at 14 mg/sec in argon, B_c changed from 600 gauss at 50 amp to less than 250 gauss at 500 amp.

Frequency Spectrum of Rotational Disturbances for $B > B_c$

The dependence of the frequency of the rotating disturbance with B for $B > B_c$ was also examined. Some of these results in argon obtained with electrostatic probes 3 in. downstream of the anode are displayed in Fig. 7. The current was constant at 300 amp. Only the dependence of the lower frequency peak (f_1) of the dual-frequency disturbance has been shown. Three mass flow conditions are examined. For all mass flow values the frequency increases with increasing B and after a sharp rise at low B becomes almost linear for $B > 2000$ gauss. Also for constant B the frequency is higher at the lower mass flow. Similar curves of frequency vs B at constant mass flow were also obtained at 400 and 500 amp; the frequency dependence showed the same behavior but the characteristic frequencies were higher at the higher currents. These results were compared with similar results given in Refs. 7 and 8. Although the geometries of the devices differ in some respects, the present results do show agreement where any comparison can be made. Similar behavior of frequency vs B with mass flow as parameter is also observed for the linear Hall accelerator.

In Fig. 7 three regimes of the arc plasma can be distinguished. First is the preonset plasma state where no rotating disturbance is present. In argon, the upper bound for this regime (B_c) depends upon mass flow, as shown in Fig. 5. Second is the postonset plasma state when the rotating disturbance is present and the noncoherent oscillations are relatively low in amplitude. At 20 mg/sec, this regime extends from B_c up to 2400 gauss, and with increasing mass flow, the upper bound on this regime occurs at higher values of B. The third regime is the postonset plasma state in which the amplitude of the noncoherent oscillations becomes comparable to the amplitude of the rotating disturbance. Figure 2d is an example of this plasma state at relatively high mass flow. For lower mass flow, the rotating disturbance was not detectable at 5500 gauss because of the amplitude of the noncoherent oscillations, and it has not yet been determined whether the rotating disturbance persists at high B or whether properties of the arc plasma are completely dominated by the noncoherent oscillations.

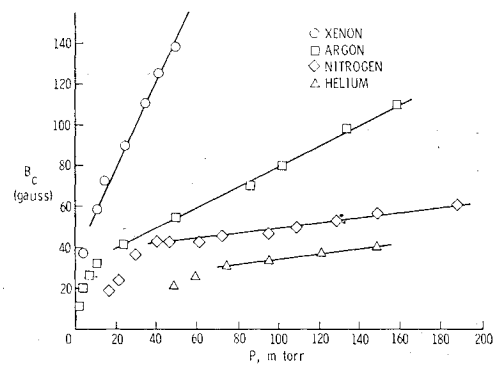

Fig. 6 Critical field vs pressure in linear Hall accelerator.

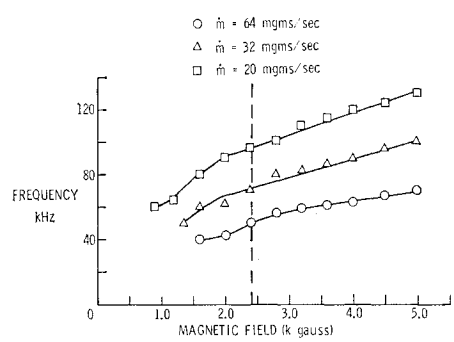

Fig. 7 Frequency of floating potential oscillations vs magnetic field using argon as propellant.

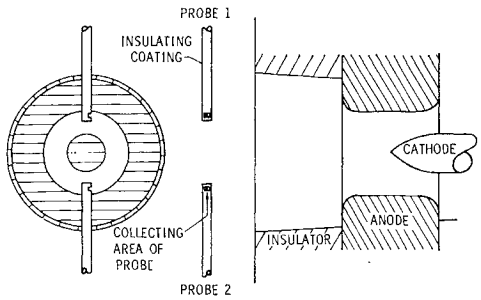

Fig. 8 Schematic of directional probes in MPD arc exhaust.

Measurement of the Ion Flux Distribution in the Exhaust Jet

The distribution of ion flux in the exhaust jet in the preonset and postonset plasma states was also observed using directional Langmuir probes biased into the ion saturation region. The orientation of these probes in the exhaust jet is shown in Fig. 8. The probes were essentially of the same construction as those described earlier with the exception that the collection area was limited to a planar circular area 12 mm^2. The centers of the two collecting areas were positioned at the same axial position on a $\frac{3}{4}$-in. radius, separated in azimuth by 180°.

In Fig. 9, the ion saturation current collected by probes 1 and 2 of Fig. 8 are shown for a bias voltage, 50 v negative with respect to the cathode. The probes were positioned 6 in. downstream of the anode. Observe that the signal on probe 1 is essentially a d.c. signal while that on probe 2 consists of a d.c. signal of approximately the same amplitude, strongly modulated by a 90-kHz a.c. signal. (The slight modulation on probe 1 was also observed on probe 2 for zero bias voltage and is probably caused by oscillations in the floating potential and not by an ion saturation current.) In Fig. 10, the effect of the direction of B on the rotating disturbance is shown. In this case, the ion flux was obtained using a single directional probe 4 in. downstream of the anode for a normal and reversed direction of B when $B > B_c$. In the reversed B direction, only a d.c. ion flux was observed but for the normal B direction, the d.c. signal is strongly modulated by the rotating disturbance. For $B < B_c$, no a.c. component was observed for either direction of B and the d.c. signals collected were of the same magnitude.

From such measurements shown in Figs. 9 and 10, it was determined that the disturbance in the ion flux rotated in the direction of $\mathbf{j} \times \mathbf{B}$ and reversed direction of rotation when B was reversed. When the ion flux signal was examined with the spectrum analyzer, the same characteristic frequencies and mode structures were observed as with the floating potential oscillations discussed earlier. Thus, the ion flux disturbance detected with the biased directional probes probably represents the same disturbance as the signals observed with floating probes.

Discussion of Thrust and Spectroscopic Measurements

Thrust measurements in argon and ammonia were also performed to determine what effect the presence or absence

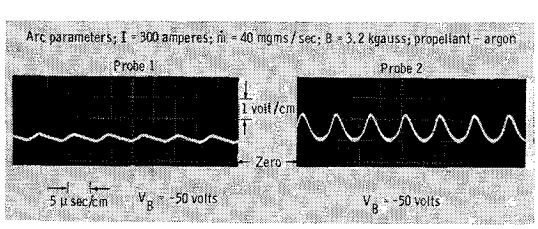

Fig. 9 Ion saturation current 6 in. downstream of anode.

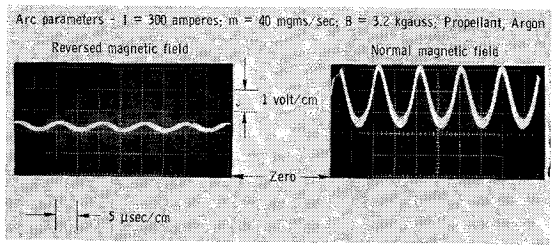

Fig. 10 Ion saturation current 4 in. downstream of anode.

of the rotating disturbance had on the thrust and to determine what effect the noncoherent oscillations (at high B) had on the thrust. In Fig. 5 the onset of the rotating disturbance is observed to depend upon mass flow for the heavier inert gases (including argon and xenon) and to show little dependence on mass flow for lighter gases (including helium, nitrogen, and ammonia). Therefore, to compare the effect of the rotating disturbance on thrust, thrust measurements were performed in a heavy propellant (argon) and in a light propellant (ammonia), for values of B ranging from 800 to 4000 gauss and for several values of mass flow.

In Fig. 11 the dependence of thrust on B is shown in argon for four values of mass flow at a constant current of 300 amp. At the lower mass flow (14 and 30 mg/sec), the thrust increases sharply at the lower values of B, but levels off in both cases at high B. At 40 and 60 mg/sec, the thrust does not level off at the higher values of B, but shows an almost linear increase from 800 to 4000 gauss.

In Fig. 12 the dependence of thrust on B is shown in ammonia for three values of mass flow. For the sake of comparison, the curve for argon at 40 mg/sec has also been included. In ammonia at the lower mass flows (14 and 20 mg/sec) the thrust becomes constant at approximately B = 2000 gauss. At the higher mass flow the thrust shows an almost linear increase with B similar to what is observed in argon.

Spectroscopic measurements of the light intensity emitted by several A II lines were also examined as a function of B three in. downstream of the anode. The A II lines examined were at 5145.36 Å, 4879.90 Å, 4806.07 Å, and 4609.60 Å. The optical system was aligned to examine light emitted along the central bright core of the device. Measurements at low mass flow ($\approx$14 mg/sec) indicate that the intensity of A II lines in the highly ionized central core of the plasma jet tends to saturate at high B like the thrust, while the intensity of A I (neutral) and A III (doubly ionized) lines does not appreciably change. This suggests that the ionization in the central core of the plasma does not appreciably increase after noncoherent oscillations appear. This speculation is further supported from measurements of ion density with increasing B, using electrostatic probes located 1 in. off the central axis. Ion density measurements in the highly ionized central core, however, could not be obtained due to excessive probe heating.

If the results in Figs. 11 and 12 showing thrust vs B are compared with results in Fig. 5 showing the dependence of B_c on mass flow, it is observed that the onset of the rotating disturbance does not correspond to an abrupt change in

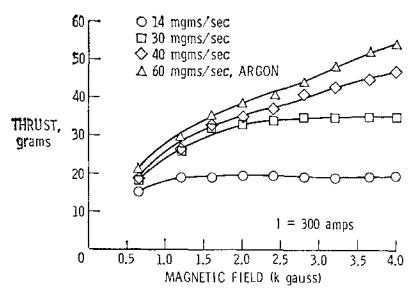

Fig. 11 Thrust vs magnetic field in argon.

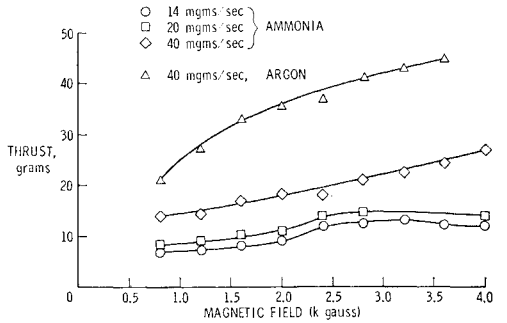

Fig. 12 Thrust vs magnetic field in ammonia.

thrust. This is not surprising if one recalls that the amplitude of the disturbance is small just above B_c. For the entire range of mass flow, the thrust increases with magnetic field after onset has set in but at low mass flow, the thrust saturates at some B less than 4000 gauss. At high mass flow, the thrust continually increases with increasing B. Ammonia and argon show similar behavior even though the dependence of B_c on mass flow differs in the two devices.

If this behavior is correlated with electrostatic probe measurements, then it is observed that noncoherent oscillations appear in the arc plasma at approximately the same values of B as when the thrust saturates. However, if noncoherent oscillations do not appear (e.g., at high mass flow), the thrust does not saturate but continues to increase with B. The saturation in thrust, at low and medium $\dot{m}$, took place even though the arc voltage (and thus the input arc power) increased with increasing B. Thus, it appears that the thrust efficiency degrades when the oscillations in the floating potential and ion flux make a transition to an apparently turbulent state and little gain in thrust efficiency is to be expected when the MPD arc is operated at relatively high B. Furthermore, spectroscopic and ion density measurements in the exhaust suggest that at low mass flow, the ionization also does not substantially increase when the noncoherent oscillations appear.

Concluding Remarks

Onset of rotating disturbances in a high-power MPD arc (15–40 kw) has been observed to occur at a critical value of magnetic field (B_c). Onset was observed to occur in both the interelectrode region and exhaust plume of the arc plasma for the same value of B_c at the cathode tip. B_c was found to depend on mass flow for the heavier inert gases (argon and xenon) but was independent of mass flow for the lighter gases (helium, nitrogen, and ammonia). The onset of the rotating disturbance suggests that it behaves more like an instability associated with conditions of the arc plasma, than a simple arc spoke normally associated with electrode phenomena. The onset of the rotating disturbance does not appear to affect the thrust efficiency of the arc since no abrupt change in thrust is observed when the plasma becomes unstable at $B = B_c$. However, when the plasma exhibits large amplitude noncoherent oscillations in the floating potential and ion flux at high B, the thrust saturates even though the input arc power is continuously going up with B. Thus, it appears that the appearance of the noncoherent oscillations can be associated with the observed degradation of thrust at high B.

References

[1] Lary, E. C., Meyerand, R. G., Jr., and Salz, F., "Fluctuations in Gyro-Dominated Plasmas," *Proceedings of the Sixth International Conference on Ionization Phenomena in Gases*, Vol. 2, Paris, July 9–13, 1963, p. 441.

[2] Hess, R. V. et al., "Study of Instabilities and Transition to Turbulent Conduction in the Presence of Hall Currents," *International Symposium on Diffusion of Plasma Across a Magnetic Field*, Institut Für Plasmaphysik, Garching Bei Munchen, Germany, 1964.

[3] Janes, G. S. and Lowder, R. S., "Anomalous Electron Diffusion and Ion Acceleration in a Low Density Plasma," *The Physics of Fluids*, Vol. 9, 1966, p. 1115.

[4] Hess, R. V. et al., "Theory and Experiments for the Role of Space-Charge in Plasma Acceleration," *Proceedings of Electromagnetics and Fluid Dynamics of Gaseous Plasma*, Vol. 11, Brooklyn, April 4–6, 1961, p. 269.

[5] Brockman, P. et al., "Diagnostic Studies in a Hall Accelerator at Low Exhaust Pressure," *AIAA Journal*, Vol. 4, No. 7, July 1966, pp. 1209–1214.

[6] Ekdahl, C., Kribal, R., and Lovberg, R., "Internal Measurements of Plasma Rotation in an MPD Arc," AIAA Paper 67-655, Colorado Springs, Colo., 1967.

[7] Larson, A., "Experiments on Current Rotations in an MPD Engine," *AIAA Journal*, Vol. 6, No. 6, June 1968, pp. 1001–1006.

[8] Connolly, D. et al., "Low Environmental Pressure MPD Arc Tests," AIAA Paper 67-685, Colorado Springs, Colo., 1967.

[9] Sidney, B. D., Hess, R. V., and Allario, F., "Onset and Suppression of Plasma Instability in Crossed-Field Geometry," *Bulletin of the American Physical Society*, Vol. 13, 1968, p. 839.

[10] Malliaris, A. C., "Oscillations in an MPD Accelerator," *AIAA Journal*, Vol. 6, No. 8, Aug. 1968, pp. 1575–1577.

[11] Shipp, J. I. and Dunnill, W. A., "Dual Frequency Instability of a Low Pressure Magnetically Confined Plasma," *Ninth Symposium on Engineering Aspects of MHD*, Univ. of Tennessee, Tulahoma, Tenn., 1968, pp. 62–69.